A Lifetime Maximization Scheme for a Sensor Based MTC Device

Sheeraz A. Alvi, Xiangyun Zhou, Salman Durrani
Research School of Engineering, The Australian National University, Canberra, ACT 2601, Australia.
Emails: {sheeraz.alvi, xiangyun.zhou, salman.durrani}@anu.edu.au.

***Abstract*—For a sensor based machine-type communication (MTC) device, transmission is a power hungry operation and blindly applying too much data compression may even exceed the cost of transmitting raw data, thus losing its purpose. Hence, it is important to investigate the trade-off between data compression and transmission energy costs. We consider a system that is composed of an energy constrained sensor based MTC device and a sink node, and devise an optimal data compression and transmission policy with an objective to maximize the lifetime of the sensor based MTC device whilst satisfying specific delay and bit error rate (BER) constraints when statistical channel gain is known at the sensor node. Our results show that a jointly optimized compression-transmission policy achieves 100% to 1500% better performance as compared to optimizing transmission only without compression under given BER and delay constraints. Importantly, the gain is most profound in the low latency regime.**

***Index Terms*—Machine-type communication, lifetime, data compression, data transmission, energy efficiency.**

I. Introduction

The Internet of things (IoT) has the potential to transform the way we live and work. However, the limited lifetime of battery operated machine-type communication (MTC) devices is holding back the potential of IoT [1]. Delivering power wirelessly to MTC devices is one possible solution, which is currently being researched [2], [3]. Another solution, which is the focus of this work and is an important complementary solution to wireless power transfer, is to intelligently design the operation of the sensor based MTC devices in order to maximize their lifetime.

The *node-lifetime* is defined as the time taken by the MTC device to deplete all of its energy. The existing literature proposes power-rate adaptation [4–8] as a solution to maximize the node-lifetime. These works consider transmission energy as a monotonically increasing function of the transmission rate. Therefore, these schemes propose to transmit data at lower transmission rates under given delay constraint to achieve energy efficiency. These schemes assume the distance between communicating devices is large, thus the transmit power dominates the circuit power [9], [10]. However, in many practical sensor networks, e.g., body area networks, the distance is fairly small and the circuit power cost cannot be ignored. This is the case particularly for smaller modulation constellation sizes, which are more common in sensor networks. Therefore, simply decreasing the transmission rate may not necessarily improve energy efficiency in practical sensor networks.

This work was supported by the Australian Research Council's Discovery Project Funding Scheme (Project number DP170100939).

In many future IoT applications, e.g., based on multimedia monitoring [11], the amount of sensed data (raw data) can sometimes be very large, resulting in high transmission cost. In this regard, data compression schemes have been proposed [12–15], which decrease the amount of data to be transmitted and thus alleviate the transmission energy cost.

Design Challenge: The transmission energy cost depends upon the compressed data size and transmission rate [9]. Furthermore, blindly applying too much compression may even exceed the cost of transmitting raw data, thereby losing its purpose [16]. Hence, it is interesting to investigate this trade-off, between data compression and transmission energy costs, to optimally utilize the energy resources in order to maximize the node-lifetime for sensor based MTC devices.

Paper contributions: We consider a monitoring system in which an energy constrained *sensor node* performs three operations: (i) data sensing, (ii) compression, and (iii) transmission to *sink node*. The sensor node devises an optimal compression and transmission policy with an objective to extend its lifetime. In this regard, we investigate the following important problem:

Problem: *What is the optimal compression and transmission policy that minimizes the compression and transmission energy cost under specific delay and bit error rate (BER) constraints?*

We study this problem in the scenario when only the statistical channel gain is known at the sensor node. Our results show that a jointly optimized compression-transmission policy performs much better than optimizing transmission only without compression under any given BER and delay constraints, particularly when the delay constraint is stringent. The optimal level of compression is insensitive to the change in the BER requirement. However, the optimal transmission rate increases as the BER constraint gets less stringent.

II. System model

We consider a system consisting of a sensor node transmitting its sensed data to a sink node, as illustrated in Fig. 1. The sensor node is battery operated and energy constrained, whereas the sink node has no energy constraint. The system follows a block-wise operation with a block of duration T, as shown in Fig. 2. Within each time block the sensor node performs three main functions, i.e., (i) sensing, (ii) compression, and (iii) transmission, each having individual completion time and energy cost.

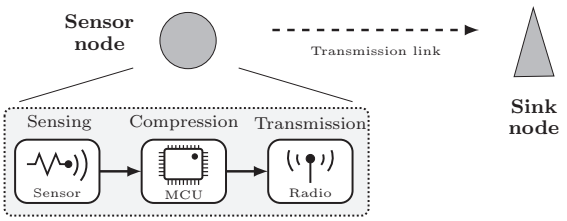

Fig. 1: Illustration of the considered system model.

For energy efficient operation, we employ radio duty cycling (RDC), i.e., the radio is kept in the sleep state except during the transmission process. Moreover, the micro-controller unit (MCU) is kept in the inactive state, when it is neither compressing nor transmitting data, usually referred to as deep sleep. The transition periods from sleep to active states and vice versa are fast enough to be negligible for both radio and MCU. We assume the power consumed by the radio and MCU is negligible during inactive states.[1]

Sensing: We consider that the data sensing can be done in parallel with the compression and transmission processes. The sensed data during a given time block, is available for transmission at the start of next time block, which is in line with prior works [5–8]. We assume that the periodic data sensing, to acquire a fixed amount of data, consumes a constant time and energy [17]. Let the time and power spent by the sensor node to sense data of size D bits be denoted by T_{sen} and P_{sen}, respectively.

Compression: Before transmission, the sensed data of size D bits is compressed into D_{cp} bits as per the given compression ratio $\frac{D_{\text{cp}}}{D}$. Let the *compression time* be denoted by T_{cp}. In this work, we adopt a non-linear compression cost model given in [18] to compute the compression time as a function of the compression ratio, $\frac{D_{\text{cp}}}{D}$, which is given as

$$T_{\text{cp}} = \tau D\big(D^{\beta} D_{\text{cp}}^{-\beta} - 1\big), \tag{1}$$

where β is the compression algorithm dependent parameter and τ is the per bit processing time. In general, β is proportional to the compression algorithm's complexity and it determines the time cost for achieving a given compression ratio for given hardware resources. β can be calculated off-line for any specified compression algorithm and given hardware resources. τ depends upon the MCU processing resources and the number of program instructions executed to process 1 bit of data. Note that τ does not represent the compression time per bit. It can be given as

$$\tau = \underbrace{\frac{\text{instructions}}{\text{program}}}_{(i)} \times \underbrace{\frac{\text{clocks}}{\text{instruction}}}_{(ii)} \times \underbrace{\frac{\text{seconds}}{\text{clock}}}_{(iii)} \times \underbrace{\frac{1}{\text{reg}}}_{(iv)}, \tag{2}$$

The explanation for the terms in (2) is as follows:

(i) We assume a single-instruction program that is able to process 1 bit of information.

[1]The inactive states power cost may affect the lifetime if T is large but won't change the compression and transmission design as shown in this work.

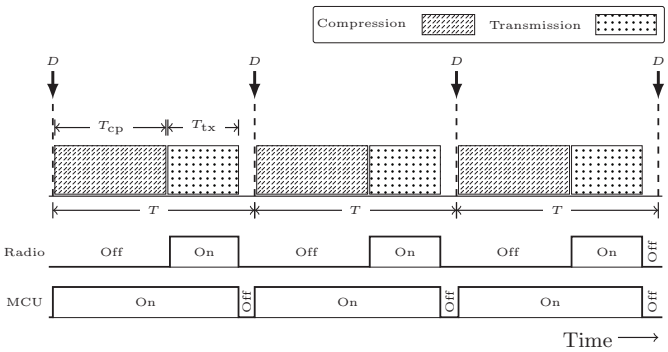

Fig. 2: Timing diagram for compression and transmission processes and corresponding radio and MCU activity cycles.

(ii) Most instructions in a typical sensor mote's MCU are executed in 1 clock cycle. We assume a single instruction is executed in 1 clock cycle.

(iii) Seconds per clock represents the clock speed, i.e., the inverse of the MCU operational frequency which typically is between few MHz to hundreds of MHz.

(iv) reg represents MCU register size. Typical sensor mote's reg is 8-bit, 16-bit or 32-bit. For a 8-bit processor, the execution time to process 1 bit or up to 8 bits is the same. We assume D is large (thousands of bits) and it will be processed in chunks of 8 bits.

Let P_{cp} denote the power consumed by the sensor node during data compression process. P_{cp} is the same as the power consumed by the MCU while processing information, which is predefined for a given sensor mote.

Transmission: Once the compression process is complete, the sensor node needs to transmit the compressed data, D_{cp}, within the next $T - T_{\text{cp}}$ seconds. The sensed data needs to be compressed and transmitted within each time block, hence the delay constraint is T seconds. Let the *transmission time* be denoted by T_{tx}. We consider the sensor node uses M-QAM modulation scheme with constellation size equal to $M = 2^l$, where $l = 1, 2, 3, .., L$. Thereby, T_{tx} is given as

$$T_{\text{tx}} = \frac{D_{\text{cp}}}{r}, \tag{3}$$

where

$$r = \frac{\log_2\left(M\right)}{T_{\text{s}}}, \tag{4}$$

where T_{s} is the symbol period.

To compute the data transmission power cost, denoted by P_{tx}, we adopt a practical model as given in [9]

$$P_{\text{tx}} = \frac{\varepsilon}{\mu} P_{\text{t}} + P_{\text{o}}, \tag{5}$$

where P_{t} is the average transmit power level, P_{o} is the communication module circuitry power, μ is the drain efficiency of the power amplifier and ε is the peak-to-average ratio (PAR) which depends upon the modulation scheme and its order. Since, we consider M-QAM modulation, ε is given as [19]

$$\varepsilon = 3\frac{\sqrt{M} - 1}{\sqrt{M} + 1}. \tag{6}$$

We assume that the battery used for sensor node possesses a limited charge storage capacity as well as a maximum current withdrawal limit. Thus, instantaneous power of any process at any state should not exceed the maximum allowable limit in order to ensure the feasibility of the system for practical systems.

Channel model: The sensor node is located at a distance d from the sink node. The channel between the two nodes is composed of a large-scale path loss, with path loss exponent α, and small-scale quasi-static flat Rayleigh fading channel, i.e., the fading channel coefficient h remains constant over a time block and is independently and identically distributed from one time block to the next. The additive noise is assumed to be AWGN with zero mean and variance σ^2.

The probability distribution function of the instantaneous channel gain, $|h|^2$, is exponentially distributed and is given as

$$f\big(|h|^2\big) \triangleq \frac{1}{\varsigma}\exp\bigg(-\frac{|h|^2}{\varsigma}\bigg), \quad |h|^2 \geqslant 0, \tag{7}$$

where ς represents the scale parameter of the probability distribution. We assume the sink node has perfect estimate of the channel but no instantaneous feedback is available. Only the statistical channel information is available at the sensor node.

Bit error rate (BER) expression: Various BER expressions exist in the literature for M-QAM. Here, we use the following BER bound defined for M-QAM [20], since it is easy to invert in order to obtain M as a function of the required BER

$$\text{BER} \leqslant \omega_2 \exp\bigg(-\frac{\omega_1}{(M-1)}\gamma\bigg), \tag{8}$$

where ω_1, ω_2 are constants and γ represents the received signal-to-noise ratio (SNR) which is defined as follows [21]

$$\gamma = \kappa\frac{P_{\text{t}}|h|^2}{\sigma^2 d^{\alpha}}, \tag{9}$$

where $\kappa = \big(\frac{\lambda}{4\pi}\big)^2$ is the attenuation factor and λ is the wavelength. For $M \geqslant 4$ and $0 \leqslant \gamma \leqslant 20$ dB, the bound in (8) with $\omega_1 = 1.5$ and $\omega_2 = 0.2$, is tight to within 1 dB of the exact result in [21].

Node Lifetime We assume that the sensor node's battery is initially fully charged. The node lifetime, denoted by T_{NL}, is defined as the time taken by the node to deplete all of its battery energy. T_{NL} can be given as

$$T_{\text{NL}} = \frac{B_{\text{cap}}V_{\text{op}}}{P_{\text{avg}}}, \tag{10}$$

where B_{cap} is the battery capacity that is the measure of the charge stored by the battery, V_{op} is the operating voltage, and P_{avg} is the average power consumed during time block T and is given as

$$P_{\text{avg}} = \frac{T_{\text{sen}}P_{\text{sen}} + \Psi}{T}, \tag{11}$$

where Ψ is the energy consumed by the compression and transmission processes within a time block which is given as

$$\Psi \;=\; T_{\text{cp}}P_{\text{cp}} + T_{\text{tx}}P_{\text{tx}}. \tag{12}$$

III. Node-Lifetime Maximization Problem

To guarantee reliable data transmission performance as per the desired QoS requirements, we specify two constraints:

1) Both compression and transmission processes are required to be completed within a delay deadline.
2) Transmission scheme is required to meet certain BER performance.

Hence, the goal is to prolong the node-lifetime, T_{NL}, for the given energy resources and QoS requirements.

In this work, the main problem we want to address is to determine the optimal compression and transmission policy which will maximize T_{NL} under given delay constraint and BER performance. From (10), we can see that T_{NL} is calculated using a predefined initial energy level, $B_{\text{cap}}V_{\text{op}}$, and the controllable rate of energy consumption, P_{avg}, which is a function of Ψ. T_{NL} is inversely proportional to Ψ, i.e., maximizing T_{NL} is equivalent to minimizing Ψ, which inherits the tradeoff between data compression and transmission.

Since only statistical channel information is available at the sensor node, thus the sensor node cannot adapt compression and transmission policy to varying channel conditions in different time blocks. Instead the sensor node needs to determine a constant compression ratio and transmission rate, and subsequently use it in each time block.

Given the fading power gain distribution, $f(|h|^2)$, the node-lifetime maximization problem can be expressed as follows

$$\begin{aligned} \underset{M,P_{\text{t}},D_{\text{cp}}}{\text{minimize}} \quad & \Psi(M, P_{\text{t}}, D_{\text{cp}}) \\ \text{subject to} \quad & T_{\text{cp}} + T_{\text{tx}} \leqslant T, \quad \mathbb{P}\{\text{BER} \leqslant \phi\} \geqslant \vartheta, \\ & M \geqslant 2, \quad P_{\text{t}} \geqslant 0, \quad D_{\text{cp}} \geqslant 0, \quad D_{\text{cp}} \leqslant D. \end{aligned} \tag{13}$$

where the first constraint in (13) defines the delay constraint for the data delivery, i.e., both compression and transmission processes should be completed within the deadline, and the second constraint in (13) mandates that the probability of having as acceptable level of BER should be greater than certain percentage. Specifically, ϕ denote the maximum acceptable BER and ϑ denote the required minimum probability of achieving the acceptable BER performance. Note that an alternative way of constraining the BER performance is to put an upper bound on the average BER over all time blocks. But we do not adopt it because it gives minimal control over the BER performance in each time block. The remaining constraints reflect practical range of values for $M, P_{\text{t}}, D_{\text{cp}}$.

In order to solve (13), we first present Proposition 1, which allows the solution to (13) to be given by Theorem 1.

Proposition 1. *The optimal P_{t} to minimize $\Psi(M, P_{\text{t}}, D_{\text{cp}})$ for given values of M and D_{cp} while satisfying the constraints in* (13) *is given by*

$$P_{\text{t}} = (M-1)\frac{\Omega}{\varsigma\ln(\vartheta)}. \tag{14}$$

where

$$\Omega = \frac{\sigma^2 d^{\alpha}\ln(\phi/\omega_2)}{\omega_1\kappa}. \tag{15}$$

Proof: The proof is provided in Appendix A. ∎

Using the result in Proposition 1, substituting T_{cp}, T_{tx}, r, P_{tx}, ε and P_{t} from (1), (3), (4), (5), (6) and (14), respectively, in (12) yields Ψ as a function of M and D_{cp}, which can be expressed as follows

$$\Psi(M, D_{\text{cp}}) = \tau D^{\beta+1} D_{\text{cp}}^{-\beta} P_{\text{cp}} - \tau D P_{\text{cp}} + \frac{D_{\text{cp}} T_{\text{s}} \ln(2)}{\ln(M)} \left(\frac{3\Omega(M^{\frac{1}{2}} - 1)^2}{\mu \varsigma \ln(\vartheta)} + P_{\text{o}} \right). \quad (16)$$

Now a simpler equivalent optimization problem with only two design parameters, i.e., M, D_{cp}, needs to be solved and the third parameter P_{t} can be obtained using the result in Proposition 1. Accordingly, the solution to the optimization problem in (13) is given by the following theorem.

Theorem 1. *In solving the optimization problem in* (13)*, the optimal constellation size is given by*

$$M^* = \begin{cases} \widetilde{M}, & \text{if } \mathcal{Q}(\widetilde{M}, \widetilde{D}_{\text{cp}}) < T. \\ \widehat{M}, & \text{otherwise.} \end{cases} \quad (17)$$

where $\widetilde{M}$ and $\widehat{M}$ are given by the solution of the following equations which can be solved numerically using VPA *method*

$$3\Omega\big(\widetilde{M}^{\frac{1}{2}} - 1\big)\big((\ln(\widetilde{M}) - 1)\widetilde{M}^{\frac{1}{2}} + 1\big) = \mu \varsigma P_{\text{o}} \ln(\vartheta), \quad (18)$$

$$\left(T + \tau D - \tau D \xi^{\frac{-\beta}{\beta+1}}\right) \ln\left(\widehat{M}\right) = D T_{\text{s}} \xi^{\frac{1}{\beta+1}} \ln(2), \quad (19)$$

where

$$\xi = \frac{P_{\text{cp}} - P_{\text{o}} + \frac{3\Omega}{\mu \varsigma \ln(\vartheta)} \big(\widehat{M}^{\frac{1}{2}} - 1\big)\big((\ln(\widehat{M}) - 1)\widehat{M}^{\frac{1}{2}} + 1\big)}{-\frac{3\Omega}{\varsigma \tau \beta \mu \ln(\vartheta)} \big(\widehat{M}^{\frac{1}{2}} - \widehat{M}\big)}, \quad (20)$$

respectively,

$$\mathcal{Q}(\widetilde{M}, \widetilde{D}_{\text{cp}}) \triangleq \tau D^{\beta+1} \widetilde{D}_{\text{cp}}^{-\beta} - \tau D + \frac{\widetilde{D}_{\text{cp}} T_{\text{s}}}{\log_2\big(\widetilde{M}\big)}, \quad (21)$$

and

$$\frac{\widetilde{D}_{\text{cp}}}{D} = \left(\frac{\tau \beta P_{\text{cp}} \ln(\widetilde{M})}{-\frac{3\Omega T_{\text{s}} \ln(2)}{\mu \varsigma \ln(\vartheta)} \big(\widetilde{M}^{\frac{1}{2}} - 1\big)^2 + P_{\text{o}} T_{\text{s}} \ln(2)} \right)^{\frac{1}{\beta+1}}, \quad (22)$$

and the optimal transmit power is given by

$$P_{\text{t}}^* = \big(M^* - 1\big) \frac{\Omega}{\varsigma \ln(\vartheta)}, \quad (23)$$

and the optimal compression ratio is given by

$$\frac{D_{\text{cp}}^*}{D} = \begin{cases} \frac{\widetilde{D}_{\text{cp}}}{D}, & \text{if } \mathcal{Q}(\widetilde{M}, \widetilde{D}_{\text{cp}}) < T. \\ \frac{\widehat{D}_{\text{cp}}}{D}, & \text{otherwise.} \end{cases} \quad (24)$$

where $\frac{\widehat{D}_{\text{cp}}}{D} = \xi^{\frac{1}{\beta+1}}$.

Proof: The proof is provided in Appendix B. ∎

Remark 1. *$\widetilde{M}$ and $\widetilde{D}_{\text{cp}}$ provide a lower bound on the optimization problem in* (13)*. $\widetilde{M}$ and $\widetilde{D}_{\text{cp}}$ are optimal design parameters when the first constraint in* (13) *is slack, i.e., $\mathcal{Q}(\widetilde{M}, \widetilde{D}_{\text{cp}}) < T$, and the other constraints are also slack. $\widehat{M}$ and $\widehat{D}_{\text{cp}}$ are optimal design parameters when all constraints in* (13) *are slack except for the first constraint.*

TABLE I: System Parameter Values

Symbol	Value	Symbol	Value	Symbol	Value
μ	0.35	V_{op}	3 V	D	20kb
ς	1	B_{cap}	9000 As	τ	0.35 ns/b
P_{cp}	24 mW	T_{s}	16 μs	β	5
P_{syn}	50 mW	ω_2	0.2	σ^2	-174 dBm
P_{fil}	2.5 mW	ω_1	1.5	ϕ	10^{-3}
P_{mix}	30.3 mW	d	20 m	T	50 ms

Remark 2. *The classical works* [5], [6] *and other related studies, which do not consider data compression, advocate that using lower transmission rates is the most energy efficient strategy. However, in our case the combined data compression and transmission rate strategy suggests that there exists a lower bound on the total energy cost of compression and transmission. In this regard, the corresponding optimal design parameters cost a finite delay, $\mathcal{Q}$. Therefore, if the required delay constraint is higher than this delay then these design parameters will maximize the lifetime and are optimal.*

Remark 3. *The optimal constellation size given by* (17) *is real valued. Thus, for practical admissibility, the transmission policy should opt to select the closest value from the available set of modulation order values. If a lower value is closer then it can only be selected if the first constraint in* (13) *is slack, else a higher value should be selected which will surely satisfy the first constraint in* (13)*. This optimal practical value, denoted by M_{pr}^*, is subsequently used to determine P_{t}^* and $\frac{D_{\text{cp}}^*}{D}$. M_{pr}^* can be given by the following conditional expression*

$$M_{\text{pr}}^* = \begin{cases} \min\left(2^L, \upsilon_1\right), & \text{if } |M^* - \upsilon_1| \leqslant |M^* - \upsilon_2| \\ & \text{and } \mathcal{Q}(\upsilon_1, \breve{D}_{\text{cp}}) < T. \\ \min\left(2^L, \upsilon_2\right), & \text{otherwise.} \end{cases} \quad (25)$$

where $\min(\cdot)$ *is the* min *operation, $|\cdot|$ represents the absolute value, 2^L is the maximum modulation order supported by the system, $\upsilon_1 = 2^{\lfloor \log_2(M^*) \rfloor}$, $\upsilon_2 = 2^{\lceil \log_2(M^*) \rceil}$, $\mathcal{Q}$ is defined in* (21)*, $\lfloor \cdot \rfloor$ and $\lceil \cdot \rceil$ is the floor and ceil operations, respectively. Note, the compressed data size $\breve{D}_{\text{cp}}$, is a function of the constellation size $2^{\lfloor \log_2(M^*) \rfloor}$.*

IV. Results

In this section, we present the numerical results to observe the performance of the proposed scheme. Unless specified otherwise, the values adopted for the system parameters are shown in Table I. To illustrate the advantage of joint optimization of data compression and transmission rate, we also consider a baseline scheme as follows. The baseline scheme considers the same system model except data compression is not employed and it maximizes the node-lifetime by optimizing transmission rate only while meeting the delay and BER constraints. The strategy followed to optimize the transmission rate policy for the baseline scheme is essentially the same as in the state of the art [4], [6], [7]. This problem can be given as in (13) by substituting $D_{\text{cp}} = D$. The optimal constellation size for this scheme, denoted by M_{nc}^*, can be obtained using Proposition 2.

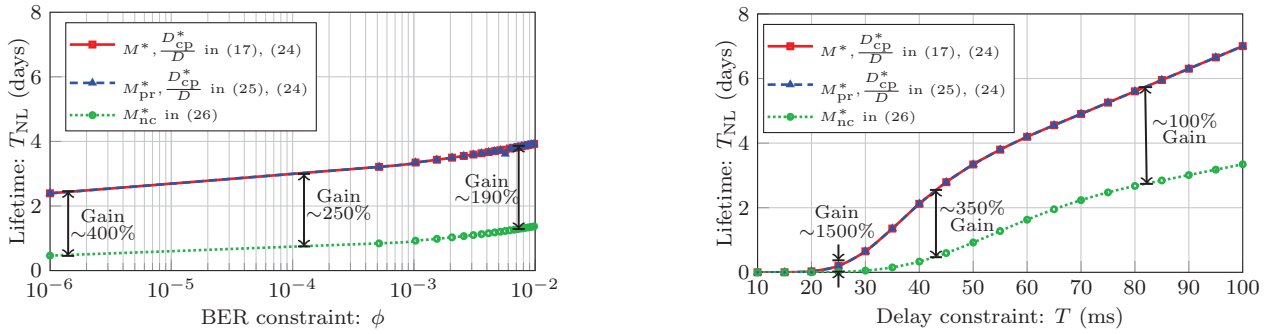

(a) (b)

Fig. 3: Lifetime vs. BER (a) and delay constraints (b), when T = 50 ms for (a) and $\phi = 10^{-3}$ for (b), and ϑ = 0.95.

Proposition 2. *The optimal constellation size to maximize lifetime without performing compression while satisfying constraints in* (13) *is given by the following conditional expression*

$$M^*_{\text{nc}} = \begin{cases} \widetilde{M}, & \text{if } \frac{DT_{\text{s}}}{\log_2\left(\widetilde{M}\right)} < T. \\ \exp\left(\frac{DT_{\text{s}}\ln(2)}{T}\right), & \text{otherwise.} \end{cases} \tag{26}$$

where $\widetilde{M}$ *is given by the solution of the following equation which can be solved numerically using the* VPA *method*

$$3\Omega\big(\widetilde{M}^{\frac{1}{2}} - 1\big)\big((\ln(\widetilde{M}) - 1)\widetilde{M}^{\frac{1}{2}} + 1\big) = \mu\varsigma P_{\text{o}}\ln(\vartheta), \tag{27}$$

and the optimal transmit power is given by

$$P^*_{\text{t}} = \big(M^*_{\text{nc}} - 1\big)\frac{\Omega}{\varsigma\ln(\vartheta)}. \tag{28}$$

Proof: The proof follows similar steps as the proof of Proposition 1 and Theorem 1, by substituting $D_{\text{cp}} = D$. Hence, it is omitted for brevity. ∎

Advantage of Proposed Scheme: Fig. 3a plots the node lifetime, T_{NL} (days), versus the BER constraint, ϕ, for system parameters in Table I. The lifetime is plotted with the optimal (real valued) M^* in (17), the practical (quantized value) ${M_{\text{pr}}}^*$ in (25) and the baseline scheme in ${M_{\text{nc}}}^*$ in (26) in Fig. 3a. We can see that the gain compared to the baseline scheme is significant - between 190% to 400% for the considered range of BER constraint. This shows the advantage of joint optimal compression and transmission rate control. In addition, we can see that the node-lifetime is not so significantly affected by the BER constraint. As the BER constraint is relaxed, the lifetime slightly increases. For instance, as BER constraint is varied from stringent BER requirement, i.e., 10^{-6}, to loose BER requirement, i.e., 10^{-2}, the lifetime only changes by around 40%. Finally, the performance with practical modulation scheme is very close to the optimal performance.

Fig. 3b plots the node lifetime, T_{NL} (days), versus the delay constraint, T (ms), for system parameters in Table I. The lifetime is plotted with the optimal (real valued) M^* in (17), the practical (quantized value) ${M_{\text{pr}}}^*$ in (25) and the baseline scheme in ${M_{\text{nc}}}^*$ in (26) in Fig. 3b. It can be seen from the figure that the lifetime is significantly affected by the delay constraint. Note that $T = 10$ ms corresponds to low latency applications, while $T = 100$ ms corresponds to application scenarios with relatively less stringent delay requirements. As before, the performance of practical modulation scheme is very close to the optimal performance.

From Fig. 3a and 3b we can say that joint optimization is much better than no compression under any BER and delay constraints. In addition, the gain is relatively larger when the delay constraint is stringent, i.e., in the low latency regime.

Impact of BER and Delay Constraints: Fig. 4a plots that for a given BER constraint, ϕ, as ϑ increases both the transmission rate and the level of compression decrease. However, in the case of stringent BER requirement, i.e., $\vartheta = 0.99$, both the level of compression and transmission rate remain almost constant for different values of ϕ. For a given value of ϑ, the level of compression increases with ϕ.

Fig. 4b shows that for a given delay constraint, as ϑ increases, the transmission rate decreases. This is because the value of the upper bound $\mathcal{Q}$ in (21) increases as ϑ increases. Thus, the level of compression increases until this upper bound value is reached and afterwards it remains almost constant.

V. Conclusion

We investigated the joint optimization of compression and transmission strategy for an energy-constrained sensor node, and illustrated their tradeoff. The joint optimization performs much better than only optimizing transmission rate without compression under any BER and delay constraints. The gain is relatively large when the delay constraint is stringent, i.e., in the low latency regime. It is best to reduce compression and increase the transmission rate when the delay constraint gets stringent and vice versa. The optimal level of compression has an inverse relationship with severity of BER requirement when the delay constraint is stringent and vice versa.

Appendix A
Proof of Proposition 1

Substituting BER constraint (8) and SNR expression (9) in second constraint in (13) yields

$$\mathbb{P}\left\{\omega_2 \exp\left(-\frac{\omega_1}{(M-1)}\frac{\kappa P_{\text{t}}|h|^2}{\sigma^2 d^\alpha}\right) \leqslant \phi\right\} \geqslant \vartheta. \tag{29}$$

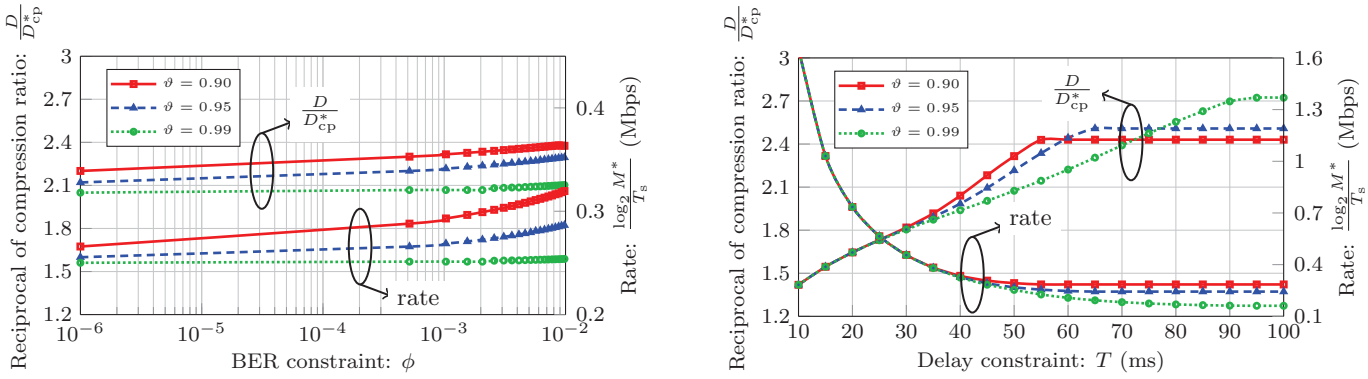

(a) (b)

Fig. 4: Optimal compression and transmission rate vs. BER (a) and delay constraints (b) for different values of ϑ, when T = 50 ms for (a) and (b) and $\phi = 10^{-3}$ for (c).

Solving (29) for fading power gain, $|h|^2$, yields

$$\mathbb{P}\left\{|h|^2 \geqslant (1-M)\frac{\sigma^2 d^\alpha \ln(\phi/\omega_2)}{\omega_1 \kappa P_{\text{t}}}\right\} \geqslant \vartheta. \tag{30}$$

The left hand side of (30) represents the complimentary cumulative distribution function (ccdf) for $|h|^2$. Since, $f\left(|h|^2\right)$ is exponentially distributed, thus (30) can be given as

$$1 - \left[1 - \frac{1}{\varsigma}\exp\left((M-1)\frac{\sigma^2 d^\alpha \ln(\phi/\omega_2)}{\varsigma\omega_1 \kappa P_{\text{t}}}\right)\right] \geqslant \vartheta. \tag{31}$$

Solving (31) for P_{t} yields

$$P_{\text{t}} \geqslant (M-1)\frac{\sigma^2 d^\alpha \ln(\phi/\omega_2)}{\varsigma\omega_1 \kappa \ln(\varsigma\vartheta)}. \tag{32}$$

Ψ is an increasing function of P_{tx} which is an increasing function of P_{t}. Hence, the best choice of P_{t} to minimize Ψ while satisfying the constraint in (32) is the minimum value obtained by setting (32) with equality. Thus, P_{t} can be given as a function of the constellation size, M, as expressed in (14).

Appendix B
Proof of Theorem 1

It can be shown that (16) is not convex in M. By substituting $M = \exp(z)$ in (16), Ψ can be equivalently defined as

$$\widetilde{\Psi}(z, D_{\text{cp}}) = \tau D^{\beta+1} D_{\text{cp}}^{-\beta} P_{\text{cp}} - \tau D P_{\text{cp}} + \frac{D_{\text{cp}} T_{\text{s}} \ln(2)}{z}\left(\frac{3\Omega(\exp(z/2)-1)^2}{\mu\varsigma\ln(\vartheta)} + P_{\text{o}}\right). \tag{33}$$

Now, the problem in (13) can be equivalently given as

$$\begin{aligned} \underset{z, D_{\text{cp}}}{\text{minimize}} \quad & \widetilde{\Psi}(z, D_{\text{cp}}) \\ \text{subject to} \quad & \tau\frac{D^{\beta+1}}{D_{\text{cp}}^{\beta}} - \tau D + \frac{D_{\text{cp}} T_{\text{s}} \ln(2)}{z} - T \leqslant 0, \\ & 2 - e^z \leqslant 0,\ -D_{\text{cp}} \leqslant 0,\ D_{\text{cp}} - D \leqslant 0. \end{aligned} \tag{34}$$

For brevity we omit the proof, however using basic calculus and with some algebraic manipulation, it can be shown that the problem in (34) is a convex optimization problem. Lagrangian function for (34) can be given as in (35) shown at the top of the next page, where $\Lambda_i \in \mathbf{\Lambda} = \{\Lambda_1, \Lambda_2, \Lambda_3, \Lambda_4\}$ is the Lagrangian multiplier associated with the ith constraint.

The Karush-Kuhn-Tucker (KKT) conditions for (34) are:

$$\begin{aligned} &\tau D^{\beta+1} D_{\text{cp}}^{-\beta} - \tau D + z^{-1} D_{\text{cp}} T_{\text{s}} \ln(2) - T \leqslant 0, \\ &2 - \exp(z) \leqslant 0, \quad -D_{\text{cp}} \leqslant 0, \quad D_{\text{cp}} - D \leqslant 0, \end{aligned} \tag{36a}$$

$$\Lambda_1 \geqslant 0, \quad \Lambda_2 \geqslant 0, \quad \Lambda_3 \geqslant 0, \quad \Lambda_4 \geqslant 0, \tag{36b}$$

$$\Lambda_1\left(\tau D^{\beta+1} D_{\text{cp}}^{-\beta} - \tau D + z^{-1} D_{\text{cp}} T_{\text{s}} \ln(2) - T\right) = 0,$$
$$\Lambda_2(2-\exp(z)) = 0, \quad \Lambda_3(-D_{\text{cp}}) = 0, \quad \Lambda_4(D_{\text{cp}} - D) = 0, \tag{36c}$$

$$\left[\frac{\partial \mathcal{L}}{\partial z} \ \frac{\partial \mathcal{L}}{\partial D_{\text{cp}}}\right]^\top = [0\ 0]^\top. \tag{36d}$$

where $[\cdot]^\top$ is the transpose operator.

Taking partial derivative of (35) with respect to z and by setting $\frac{\partial \mathcal{L}}{\partial z} = 0$ and after some simplification we get

$$-\frac{3\Omega T_{\text{s}}}{\mu\varsigma\ln(\vartheta)}\left(\exp(z/2)-1\right)\left((z-1)\exp(z/2)+1\right) + T_{\text{s}} P_{\text{o}} + \Lambda_1 T_{\text{s}} + \frac{\Lambda_2 z^2 \exp(z)}{D_{\text{cp}}\ln(2)} = 0. \tag{37}$$

Taking partial derivative of (35) with respect to D_{cp} and setting $\frac{\partial \mathcal{L}}{\partial D_{\text{cp}}} = 0$ and after some simplification we get

$$-\frac{z\tau\beta D^{\beta+1} D_{\text{cp}}^{-\beta-1} P_{\text{cp}}}{\ln(2)} - \frac{3\Omega T_{\text{s}}}{\mu\varsigma\ln(\vartheta)}\left(\exp(z/2)-1\right)^2 + T_{\text{s}} P_{\text{o}} + \Lambda_1\left(T_{\text{s}} - \frac{z\tau\beta D^{\beta+1} D_{\text{cp}}^{-\beta-1}}{\ln(2)}\right) - \frac{\Lambda_3 z}{\ln(2)} + \frac{\Lambda_4 z}{\ln(2)} = 0. \tag{38}$$

From (36c) we know either Λ_i is zero or the associated constraint function is zero for any given i. First we consider one of the possible cases that is Λ_1, Λ_2, Λ_3, Λ_4 do not exist. Accordingly, plugging in $\Lambda_1 = 0, \Lambda_2 = 0, \Lambda_3 = 0, \Lambda_4 = 0$ in (37), (38) yields following expressions, respectively,

$$\frac{3\Omega}{\mu\varsigma\ln(\vartheta)}\left(\exp(z/2)-1\right)\left((z-1)\exp(z/2)+1\right) = P_{\text{o}}, \tag{39}$$

$$\begin{aligned}\mathcal{L}(z, D_{\text{cp}}, \mathbf{\Lambda}) \;&=\; \tau D^{\beta+1} D_{\text{cp}}^{-\beta} P_{\text{cp}} - \tau D P_{\text{cp}} + z^{-1} D_{\text{cp}} T_{\text{s}} \ln(2) \Big(\frac{3\Omega}{\mu_{\text{S}} \ln(\vartheta)} (\exp(z/2) - 1)^2 + P_{\text{o}} \Big) \\ &\quad + \Lambda_1 \Big(\tau D^{\beta+1} D_{\text{cp}}^{-\beta} - \tau D + z^{-1} D_{\text{cp}} T_{\text{s}} \ln(2) - T \Big) + \Lambda_2 (2 - \exp(z)) + \Lambda_3 (-D_{\text{cp}}) + \Lambda_4 (D_{\text{cp}} - D),\end{aligned} \tag{35}$$

$$\frac{z\tau\beta D^{\beta+1} P_{\text{cp}}}{D_{\text{cp}}^{\beta+1} T_{\text{s}} \ln(2)} + \frac{3\Omega}{\mu_{\text{S}} \ln(\vartheta)} \big(\exp(z/2) - 1\big)^2 = P_{\text{o}}. \tag{40}$$

Solving (40) for D_{cp} yields

$$\frac{D_{\text{cp}}}{D} = \left(\frac{z\tau\beta P_{\text{cp}}}{-\frac{3\Omega T_{\text{s}} \ln(2)}{\mu_{\text{S}} \ln(\vartheta)} \big(\exp(z/2) - 1\big)^2 + P_{\text{o}} T_{\text{s}} \ln(2)} \right)^{\frac{1}{\beta+1}}. \tag{41}$$

Numerically solving (39) for z yields its value $\tilde{z}$. Substituting this value of z in (41) and solving for D_{cp} yields its value $\widetilde{D}_{\text{cp}}$. $\tilde{z}$ and $\widetilde{D}_{\text{cp}}$ provide a lower bound on problem in (34). It can be shown that $\tilde{z}$ and $\widetilde{D}_{\text{cp}}$ satisfy all the KKT conditions. Hence, the derived solution in (39) and (41) is the optimal solution for (34), when all constraints are slack.

Now consider that Λ_1 exits and $\Lambda_2, \Lambda_3, \Lambda_4$ do not exist. Accordingly, plugging in $\Lambda_1 \neq 0, \Lambda_2 = 0, \Lambda_3 = 0, \Lambda_4 = 0$ in (36c), (37), and (38) yields following expressions, respectively,

$$\tau D^{\beta+1} D_{\text{cp}}^{-\beta} - \tau D + z^{-1} D_{\text{cp}} T_{\text{s}} \ln(2) - T = 0, \tag{42}$$

$$-\frac{3\Omega \big(\exp(z/2) - 1\big)\big((z-1)\exp\big(z/2\big) + 1\big)}{\mu_{\text{S}} \ln(\vartheta)} = P_{\text{o}} + \Lambda_1, \tag{43}$$

$$\begin{aligned}\Lambda_1 \Big(1 - \frac{z\tau\beta D^{\beta+1} D_{\text{cp}}^{-\beta-1}}{T_{\text{s}} \ln(2)}\Big) - \frac{z\tau\beta D^{\beta+1} D_{\text{cp}}^{-\beta-1} P_{\text{cp}}}{T_{\text{s}} \ln(2)} + P_{\text{o}} \\ - \frac{3\Omega}{\mu_{\text{S}} \ln(\vartheta)} \big(\exp(z/2) - 1\big)^2 = 0.\end{aligned} \tag{44}$$

Solving (43) for Λ_1 and substituting its value in (44) yields

$$D_{\text{cp}} = D\zeta^{\frac{1}{\beta+1}} \tag{45}$$

where

$$\zeta = \frac{P_{\text{cp}} - P_{\text{o}} + \frac{3\Omega}{\mu_{\text{S}} \ln(\vartheta)} \big(\exp(z/2) - 1\big)\big((z-1)\exp(z/2) + 1\big)}{-\frac{3\Omega}{\tau\beta\mu_{\text{S}} \ln(\vartheta)} \big(\exp(z/2) - \exp(z)\big)}.$$

Substituting D_{cp} from (45) in (42) yields

$$TD^{-1} + \tau - \tau\zeta^{\frac{-\beta}{\beta+1}} = z^{-1} T_{\text{s}} \ln(2) \zeta^{\frac{1}{\beta+1}}. \tag{46}$$

Numerically solving (46) for z yields its value $\hat{z}$. Substituting this value of z in (45) and solving for D_{cp} yields its value $\widehat{D}_{\text{cp}}$. It can be shown that $\hat{z}$ and $\widehat{D}_{\text{cp}}$ satisfy all the KKT conditions. Hence, (45) and (46) is the optimal solution for (34), when all constraints are slack except the first constraint. All other cases violate one or more KKT conditions.

Finally, the optimal values of M and D_{cp} for both cases can be obtained by substituting $z = \ln(M)$ in (39), (41) and (46), (45), respectively, which will minimize the objective function in (13). Finally, by substituting the optimal value of M in (14) we can determine the optimal P_{t} which will minimize Ψ.

REFERENCES

[1] H. Yetgin, K. T. K. Cheung, M. El-Hajjar, and L. H. Hanzo, "A survey of network lifetime maximization techniques in wireless sensor networks," *IEEE Commun. Surveys Tuts.*, vol. 19, no. 2, pp. 828–854, Jan. 2017.

[2] K. Huang and X. Zhou, "Cutting the last wires for mobile communications by microwave power transfer," vol. 53, no. 6, pp. 86–93, Jun. 2015.

[3] D. N. K. Jayakody, J. Thompson, S. Chatzinotas, and S. Durrani, *Wireless Information and Power Transfer: A New Paradigm for Green Communications*. Springer International Publishing AG, 2017.

[4] W. Xu, Q. Shi, X. Wei, Z. Ma, X. Zhu, and Y. Wang, "Distributed optimal rate-reliability-lifetime tradeoff in time-varying wireless sensor networks," *IEEE Trans. Wireless Commun.*, vol. 13, no. 9, pp. 4836–4847, Sep. 2014.

[5] E. Uysal-Biyikoglu, B. Prabhakar, and A. E. Gamal, "Energy-efficient packet transmission over a wireless link," *IEEE/ACM Trans. Netw.*, vol. 10, no. 4, pp. 487–499, Aug. 2002.

[6] M. A. Antepli, E. Uysal-Biyikoglu, and H. Erkal, "Optimal packet scheduling on an energy harvesting broadcast link," *IEEE J. Sel. Areas Commun.*, vol. 29, no. 8, pp. 1721–1731, Sep. 2011.

[7] M. A. Zafer and E. Modiano, "A calculus approach to energy-efficient data transmission with quality-of-service constraints," *IEEE/ACM Trans. Netw.*, vol. 17, no. 3, pp. 898–911, Jun. 2009.

[8] M. Gregori and M. Payaro, "Energy-efficient transmission for wireless energy harvesting nodes," *IEEE Trans. Wireless Commun.*, vol. 12, no. 3, pp. 1244–1254, Mar. 2013.

[9] S. Cui, A. J. Goldsmith, and A. Bahai, "Energy-constrained modulation optimization," *IEEE Trans. Wireless Commun.*, vol. 4, no. 5, pp. 2349–2360, Sep. 2005.

[10] G. Y. Li, Z. Xu, C. Xiong, C. Yang, S. Zhang, Y. Chen, and S. Xu, "Energy-efficient wireless communications: tutorial, survey, and open issues," *IEEE Wireless Commun. Mag.*, vol. 18, no. 6, pp. 28–35, Dec. 2011.

[11] S. A. Alvi, B. Afzal, G. A. Shah, L. Atzori, and W. Mahmood, "Internet of multimedia things: Vision and challenges," *Ad Hoc Networks*, vol. 33, pp. 87–111, Oct. 2015.

[12] T. Srisooksai, K. Keamarungsi, P. Lamsrichan, and K. Araki, "Practical data compression in wireless sensor networks: A survey," *Journal of Network and Computer Applications*, vol. 35, no. 1, pp. 37 – 59, 2012.

[13] P. Kasirajan, C. Larsen, and S. Jagannathan, "A new data aggregation scheme via adaptive compression for wireless sensor networks," *ACM Trans. Sen. Netw.*, vol. 9, no. 1, pp. 5:1–5:26, 2012.

[14] X. Deng and Y. Yang, "Online adaptive compression in delay sensitive wireless sensor networks," *IEEE Trans. Comput.*, vol. 61, no. 10, pp. 1429–1442, Oct. 2012.

[15] Y. Wang, D. Wang, X. Zhang, J. Chen, and Y. Li, "Energy-efficient image compressive transmission for wireless camera networks," *IEEE Sensors J.*, vol. 16, no. 10, pp. 3875–3886, May 2016.

[16] C. M. Sadler and M. Martonosi, "Data compression algorithms for energy-constrained devices in delay tolerant networks," in *Proc. SENSYS*. ACM, Nov. 2006, pp. 265–278.

[17] S. Mao, M. H. Cheung, and V. W. S. Wong, "Joint energy allocation for sensing and transmission in rechargeable wireless sensor networks," *IEEE Trans. Veh. Technol.*, vol. 63, no. 6, pp. 2862–2875, Jul. 2014.

[18] M. Tahir and R. Farrell, "A cross-layer framework for optimal delay-margin, network lifetime and utility tradeoff in wireless visual sensor networks," *Ad Hoc Networks*, vol. 11, no. 2, pp. 701–711, Mar. 2013.

[19] H. Meyr, M. Moeneclaey, and S. Fechtel, *Digital Communication Receivers: Synchronization, Channel Estimation, and Signal Processing*. New York, NY, USA: John Wiley & Sons, Inc., 1997.

[20] G. Foschini and J. Salz, "Digital communications over fading radio channels," *The Bell System Technical Journal*, vol. 62, no. 2, pp. 429–456, Feb. 1983.

[21] A. Goldsmith, *Wireless communications*. Cambridge University Press, Aug. 2005.